An Inverse Substrate Orientation for the Regioselective Acylation of 3′,5′-Diaminonucleosides Catalyzed by *Candida antarctica* lipase B?

Iván Lavandera,[a, b] Susana Fernández,[a] Julia Magdalena,[a] Miguel Ferrero,[a] Romas J. Kazlauskas,*[b, c] and Vicente Gotor*[a]

Candida antarctica *lipase B (CAL-B) catalyzes the regioselective acylation of natural thymidine with oxime esters and also the regioselective acylation of an analogue, 3′,5′-diamino-3′,5′-dideoxythymidine with nonactivated esters. In both cases, acylation favors the less hindered 5′-position over the 3′-position by upto 80-fold. Computer modeling of phosphonate transition-state analogues for the acylation of thymidine suggests that CAL-B favors acylation of the 5′-position because this orientation allows the thymine ring to bind in a hydrophobic pocket and forms stronger key hydrogen bonds than acylation of the 3′-position. On the other hand, computer modeling of phosphonamidate analogues of the transition states for acylation of either the 3′- or 5′-amino groups in 3′,5′-diamino-3′,5′-dideoxythymidine shows similar orientations and hydrogen bonds and, thus, does not explain the high regioselectivity. However, computer modeling of inverse structures, in which the acyl chain binds in the nucleophile pocket and vice versa, does rationalize the observed regioselectivity. The inverse structures fit the 5′-, but not the 3′-intermediate thymine ring, into the hydrophobic pocket, and form a weak new hydrogen bond between the O-2 carbonyl atom of the thymine and the nucleophile amine only for the 5′-intermediate. A water molecule might transfer a proton from the ammonium group to the active-site histidine. As a test of this inverse orientation, we compared the acylation of thymidine and 3′,5′-diamino-3′,5′-dideoxythymidine with butyryl acyl donors and with isosteric methoxyacetyl acyl donors. Both acyl donors reacted at equal rates with thymidine, but the methoxyacetyl acyl donor reacted four times faster than the butyryl acyl donor with 3′,5′-diamino-3′,5′-dideoxythymidine. This faster rate is consistent with an inverse orientation for 3′,5′-diamino-3′,5′-dideoxythymidine, in which the ether oxygen atom of the methoxyacetyl group can form a similar hydrogen bond to the nucleophilic amine. This combination of modeling and experiments suggests that such lipase-catalyzed reactions of apparently close substrate analogues like alcohols and amines might follow different pathways.*

Introduction

Due to the cleanness, simplicity, and efficiency of enzymatic reactions, they are often the best route to complex molecules such as nucleoside analogues,[1] which are drug candidates for several diseases.[2] For example, pyrimidine nucleoside derivatives show antiviral[3] and antitumor[4] activities. Modifications of the sugar moiety are important sources of new compounds with promising chemotherapeutic properties.[5] One example for sugar modifications is the lipase-catalyzed regioselective acylation of natural 2′-deoxy- and ribonucleosides with vinyl[6a] and oxime esters[6b–g] or 3′,5′-diamino-2′,3′,5′-trideoxynucleosides by using nonactivated esters.[7] One of the most useful lipases, *Candida antarctica* lipase B (CAL-B), shows high regioselectivity for the functional group at the ribose 5′ position. The molecular basis of this regioselectivity is the focus of this paper.

Lipases, which normally catalyze hydrolysis of lipids, also catalyze the acylation of alcohols and amines in organic solvents.[8] Their reaction mechanism involves a Ser-His-Asp(Glu) catalytic triad,[9] in which five or six key hydrogen bonds are critical to catalysis. X-ray structures of transition-state analogues as well as molecular modeling show that formation of these hydrogen bonds defines the orientation of the substrate in the active site.[10] The acyl group binds in a large hydrophobic pocket in lipases, while the nucleophile (usually an alcohol or amine) binds in a smaller pocket, called a medium hydro-

[a] *Dr. I. Lavandera, Dr. S. Fernández, Dr. J. Magdalena, Prof. M. Ferrero, Prof. V. Gotor*
Departamento de Química Orgánica e Inorgánica
Facultad de Química, Universidad de Oviedo
33071 Oviedo (Spain)
Fax: (+34) 98-510-3448
E-mail: vgs@fq.uniovi.es

[b] *Dr. I. Lavandera, Prof. R. J. Kazlauskas*
Department of Chemistry, McGill University
Montréal, Québec, H3A 3K6 (Canada)
E-mail: rjk@umn.edu

[c] *Prof. R. J. Kazlauskas*
Current address:
Department of Biochemistry, Molecular Biology and Biophysics and The Biotechnology Institute, University of Minnesota
Saint Paul, MN 55108 (USA)
Fax: (+1) 612-625-5780

Supporting information for this article is available on the WWW under http://www.chembiochem.org or from the author.

 DOI: 10.1002/cbic.200400422

phobic pocket. Parts of a large nucleophile might extend into the large hydrophobic pocket or point into the solvent.

However, substantial experimental evidence also suggests that serine hydrolases can tolerate an inverse orientation, in which the acyl group binds in the nucleophile site and the nucleophile binds in the acyl-group site. One line of evidence is the use of "inverse substrates" of proteases. For example, trypsin favors the hydrolysis of peptides with Arg in the acyl portion of the substrate, but also catalyzes the hydrolysis of esters of *p*-amidinophenol or 4-guanidinophenol, in which the arginine side-chain mimic is in the alcohol moiety (Scheme 1).[11]

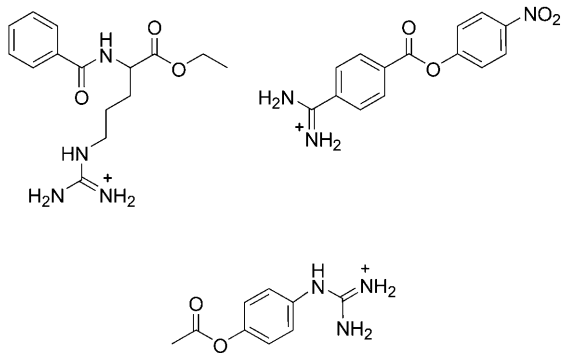

Scheme 1. Normal (top) and inverse (bottom) ester substrates for trypsin. Normal ester substrates for trypsin contain a guanidinium or amidino group in the acyl portion. However, trypsin also accepts esters of 4-guanidinophenol, in which the guanidinium group is in the alcohol moiety. The most likely explanation is that the ester reacts in an inverse orientation.

Bordusa and co-workers exploited this inverse-substrate idea to overcome the narrow substrate specificity of trypsin.[12] Instead of accepting only peptides with Arg in the acyl portion, trypsin accepted a wide range of acyl groups when Bordusa and coworkers used esters of 4-guanidinophenol. They suggest that the broadened substrate range stems from the inverse orientation, which places the 4-guanidinophenyl group in the amidino-moiety-requiring acyl-group site and the diverse acyl groups in the less structurally demanding nucleophile-binding site.[13] Recently, this group extended the same idea to clostripapain,[14] which has a similar specificity to trypsin, and also to the Glu-specific V8 protease.[15] Another line of evidence for inverse binding of substrates comes from the inhibition of acetylcholine esterase with P-chiral methylphosphonates (nerve agents). Both enantiomers inhibit this enzyme, but bind differently because of their different configuration at the phosphorus atom. The slow-reacting enantiomer binds in the inverse orientation.[16] Inhibition of lipases by carbamates might also involve such reverse binding.[17] Finally, the X-ray crystal structure of CAL-B containing a phosphonate transition-state analogue unexpectedly showed an inverse orientation.[18] Thus, there is a strong evidence that transition-state analogues can bind in an inverse orientation and that substrates can both bind and react in an inverse orientation.

Although the use of enzymes in synthesis is common, the basis of their selectivity is not well understood. The aim of this study is to identify the molecular basis of the 5′-regioselectivity of CAL-B toward nucleosides and their analogues by using computer modeling. This modeling suggests that the acylation of natural nucleosides favors the 5′-position because this orientation allows the thymine base to bind in a large hydrophobic pocket. On the other hand, modeling suggests that acylation of diaminonucleosides proceeds via an inverted substrate orientation and regioselectivity stems from better binding of the thymine ring when the 5′-amino group reacts and from a stabilizing interaction between the O-2 carbonyl group of the base and the 5′-amine nucleophile.

Results

Regioselective CAL-B-catalyzed acylation of thymidine

We previously reported CAL-B-catalyzed acylations of nucleosides with good 5′-selectivity using oxime esters as the acyl donor and tetrahydrofuran (THF) as the solvent (Scheme 2, X = O).[6b–g] The selectivity was similar for adenine, thymidine, guanidine, and cytidine,[6] so we focused on the simplest one—thymidine—in this study. We tested five acetonoxime esters as acylating agents: three with an aliphatic acyl chain (R = Me, Pr, Non) and two with acyl chains containing aromatic rings (R = Ph, CH_2Ph; Table 1). We used dry THF because previous work showed that the regioselectivity was highest in this solvent.[19]

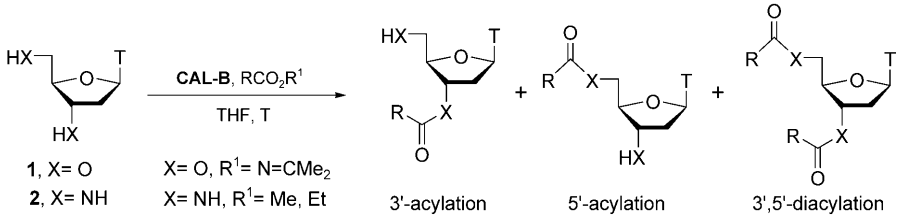

Scheme 2. Regioselective CAL-B-catalyzed acylation of thymidine (**1**) and 3′,5′-diamino-3′,5′-dideoxythymidine (**2**; T = thymine).

For the oxime esters with aliphatic acyl chains the regioselectivities were moderate (2.7:1 for acetyl, 6.4:1 for butanoyl and 4:1 for decanoyl; entries 1–3, Table 1). The acylation was complete in 4–6.5 h for acetyl and butanoyl, respectively, but required 53.5 h for decanoyl. For the oxime esters with an aromatic ring in the acyl chain, the regioselectivity was higher (>12:1 and >45:1), but the rate was very slow at 30 °C (12–45 % conversion after 37–39 h; entries 4 and 6, Table 1). At 60 °C, the regioselectivity remained high (40:1 and >75:1) and the conversions increased to 41 and 75 % for benzoyl and phenylacetyl, respectively, in shorter reaction times (6–30 h; entries 5 and 7, Table 1).

Table 1. Regioselectivity of CAL-B-catalyzed acylation of thymidine (**1**) with oxime esters.[a]

	Acyl group	R	*T* [°C]	*t* [h][b]	Conversion [%]	3′ [%]	5′ [%]	3′,5′ [%]	5′ Selectivity[c]
1	acetyl	Me	30	4	98	17	68	13	2.7:1
2	butanoyl	Pr	30	6.5	94	11	81	2	6.4:1
3	decanoyl	Non	30	53.5	99	20	79	0	4:1
4	benzoyl	Ph	30	39	12	0	12	0	>12:1
5	benzoyl	Ph	60	30	41	1	40	0	40:1
6	phenylacetyl	Bn	30	37	45	0	45	0	>45:1
7	phenylacetyl	Bn	60	6	75	0	75	0	>75:1

[a] Reactions were monitored by gas chromatography, except for the acetylation reaction. In this case, peaks of the acetylation products overlapped on GC chromatograms, so the reactions were monitored by HPLC. [b] Time refers to either the time to reach high conversions or the time after which no further reaction was observed. [c] Selectivity was estimated from the ratio of the 3′- and 5′-monoacylated products plus the amount of double acylation added to each.

Molecular modeling of the CAL-B-catalyzed acylation of thymidine

To explain the regioselectivities of CAL-B for the 5′-OH group of thymidine, we used computer modeling starting from an X-ray crystal structure of CAL-B. We modeled phosphonate analogues of the transition state for butanoylation of thymidine at both the 5′ and 3′ positions. The starting point for modeling was a simple phosphonate, which mimics the transition state for butanoylation of ethanol (Scheme 3, R = *n*-C_3H_7).[18] Geometry optimization of this simple phosphonate formed all six essential hydrogen bonds for catalysis. To model the nucleoside substrates, we added the ribose and thymine rings and systematically searched for catalytically productive conformations (see Supporting Information). We defined catalytically productive conformations as those that: a) contained all six key catalytic hydrogen bonds, b) avoided steric clashes between the phosphonate and the lipase, and c) avoided steric clashes within the phosphonate.

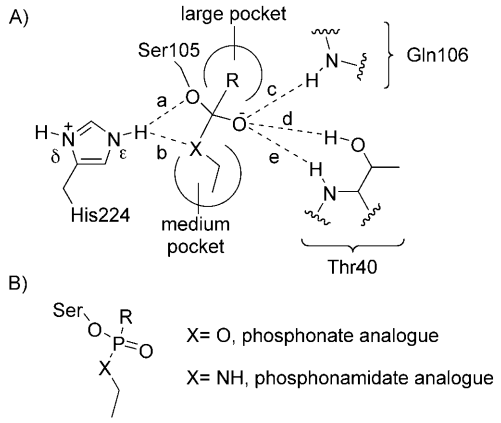

Scheme 3. Tetrahedral intermediates for the acylation of ethanol (X = O) or ethylamine (X = NH) in the normal orientation and the corresponding phosphonate (X = O) or phosphonamidate (X = NH) transition-state analogues. A) Key hydrogen bonds between CAL-B and the tetrahedral intermediate are: two from N_ε of His224 to the oxygen atom of Ser105 (a) and the XEt group of the tetrahedral intermediate (b; X = O, NH), and three from the oxyanion to Gln106 (c) and to Thr40 (d, e). A sixth key hydrogen bond is from N_δ of His224 to the carboxylate of Asp187 (not shown). B) Phosphonate (X = O) or phosphonamidate (X = NH) analogues mimick these tetrahedral intermediates in computer modeling. Further, the XEt groups are replaced by either the 5′- or 3′-nucleoside in a stepwise fashion as described in the text.

The active site of CAL-B restricts the possible orientations for the nucleoside (Figure 1).[20] Viewed with the catalytic triad Asp-His-Ser oriented from left to right, it contains a large hydrophobic pocket above the Asp-His-Ser triad and a medium-size pocket below it. In the normal orientation, the acyl moiety of the substrate lies in the large hydrophobic pocket, while the alcohol (nucleophile) moiety lies in the medium pocket, but might extend into the solvent and/or into the large hydrophobic pocket. The large hydrophobic pocket in CAL-B is lined by Ile189 and Val190 on the left, Val154 on the far right, as well as Leu140 and Leu144 at the top. Deep in this pocket, Asp134 is on the left and Gln157 on the right. The medium pocket is below the catalytic Ser105 and is crowded by Trp104 below it and the Leu278–Ala287 helix to the right. It has little room for substituents larger than propyl; several carbon atoms of the bound nucleoside lie in this region, but most of the nucleoside

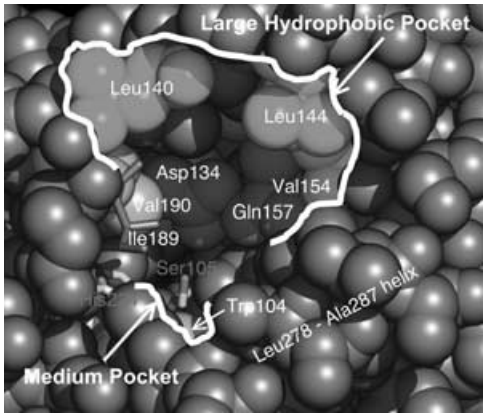

Figure 1. CAL-B active-site structure from X-ray crystallography viewed with the catalytic triad Asp-His-Ser oriented from left to right (Asp187 is hidden). The acyl group of the substrate binds first in the large hydrophobic pocket. This usually situates the substrate with the acyl group above the catalytic triad and the leaving group, or the nucleophile, below the catalytic triad. The active site contains a large hydrophobic pocket above the catalytic residues and a medium-sized pocket below. There is very little room for large substituents below the active site of CAL-B. The above image displays Ile189 in a stick representation to allow a better view of the large pocket of the lipase.

extends out into the solvent or the large hydrophobic pocket (see below).

5′ butanoylation catalyzed by CAL-B (favored): The best model of the tetrahedral intermediate of the 5′-*O*-butanoylation (Figure 2A),[21] orients the thymine in the right side of the large hydrophobic pocket above Gln157, with all six key hydrogen bonds and no intra- or intermolecular steric clashes (entry 1, Table 2).

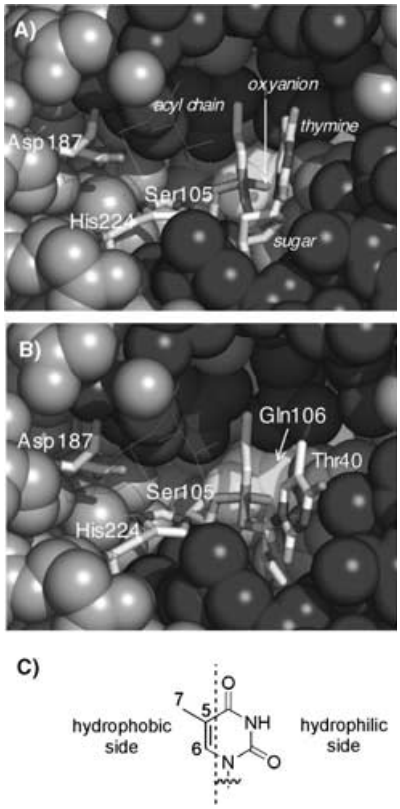

Figure 2. The best conformations of A) 5′- and B) 3′-butyrated intermediates of thymidine in CAL-B and C) hydrophobic and hydrophilic moieties of the thymine ring. The tetrahedral intermediate for the favored 5′-acylation reaction (A) situates the thymine ring on the right side of the large hydrophobic pocket, making it the most productive conformation due to better enzyme–substrate interaction. The tetrahedral intermediate for the 3′-acylation reaction (B) situates the thymine ring outside the hydrophobic pocket. The binding thymine ring appears to be the key factor to explain the enzyme regioselectivity. Darker spheres indicate the amino acids that are the limits of the medium and large hydrophobic size pockets around the CAL-B active site (see Figure 1). The above image displays Glu188 and Ile189 in a line representation to allow a better view of the large pocket of the lipase.

The hydrophobic side of the thymine ring (C-5–C-7) lies close to other hydrophobic groups (Figure 2C): the side chains of Val154, Ile189 and Ile285, and the propyl group of the acyl portion. Thus, C-6 of the thymine ring is 3.94 Å far away from C-α of the acyl chain, C-5 5.42 Å from C-β, and C-7 (methyl group of thymine) 4.08 Å from C-γ. The hydrophilic side of the thymine ring points toward the solvent, but also lies near the hydrophobic methyl group of Ala282.

Table 2. Key hydrogen-bond angles and distances in the CAL-B-catalyzed acylation of thymidine and 3′,5′-diaminothymidine.

	Figure[a]	H-bond distance [Å] (angle)[b]				
		a	*b*	*c*	*d*	*e*
1	2A	3.05 (124°)	3.08 (164°)	2.92 (157°)	2.75 (166°)	2.87 (172°)
2	2B	3.17 (131°)	2.87 (159°)	3.11 (163°)	2.78 (159°)	2.74 (164°)
3	S2	2.91 (153°)	3.25 (125°)	3.27 (160°)	2.77 (163°)	2.88 (157°)
4	S3	3.23 (141°)	3.14 (144°)	3.14 (160°)	2.75 (164°)	2.74 (159°)
5	3A[c]	–[d]	–[d]	3.14 (160°)	2.76 (152°)	2.73 (148°)
6	S4	–[d]	–[d]	3.22 (161°)	2.78 (151°)	2.77 (112°)
7	4[e]	–[d]	–[d]	3.11 (159°)	2.75 (152°)	2.75 (150°)
8	S5[c]	–[d]	–[d]	3.06 (163°)	2.79 (152°)	2.70 (145°)
9	3C[f]	–[d]	–[d]	3.09 (163°)	2.77 (152°)	2.71 (147°)

[a] See the text. [b] Scheme 3 defines the hydrogen bonds. Distances are between nonhydrogen atoms (N–N, N–O, O–O), and angles refer to the N–H–O or similar. [c] In this Figure a new short distance between the O-2 carbonyl atom of the thymine and the 5′-N nucleophile appears. Figure 3A: 3.36 Å (126°); Figure S5 in the Supporting Information: 3.13 Å (111°). [d] Not relevant because of inverse orientation of substrate, since distances are more than 4 Å. [e] Distance between the O-2 carbonyl atom of the thymine and the 5′-N nucleophile: 3.41 Å (127°); distance between the water oxygen atom and the 5′-N nucleophile: 4.13 Å (111°); distance between the water oxygen atom and the N_ε-histidine: 5.28 Å. [f] Distance between the O-2 carbonyl atom of the thymine and the 5′-N nucleophile: 3.14 Å (118°); distance between the methoxyacetyl oxygen atom and the N-5′ nucleophile: 2.54 Å (100°); distance between the methoxyacetyl oxygen atom and the N_ε-histidine: 3.21 Å.

3′ butanoylation catalyzed by CAL-B (not favored): The *trans* orientation of the 3′-alcohol and thymine prevents placing the thymine ring in the large pocket and extends it beyond the medium pocket, preventing binding there as well. The best structure has the thymine ring lying partly on the protein surface having some van der Waals contacts with the enzyme (entry 2, Table 2; Figure 2B). In this conformation, the thymine ring lies on the lower right edge of the large hydrophobic pocket with the hydrophobic side of the thymine ring near the side chains of Ile189 and Ile285. The 5′-OH group of this structure rested in the small area below the catalytic Ser105, between His224, Trp104 and Leu278. In addition to the inability to bind the thymine ring in the hydrophobic pocket, this structure contains two destabilizing interactions. First, the hydrophilic side of thymine lies near the hydrophobic side chains of Ala282 and Leu278 and O-2 of thymidine is near the carbonyl oxygen atom of Leu278. Second, it lacks a hydrophobic interaction between the propyl acyl chain and the hydrophobic side of the thymine (C-6 of the thymine ring is 5.19 Å away from the C-α atom of the acyl chain, C-5 7.43 Å from C-β, and C-7 (methyl group of thymine) 6.83 Å from C-γ). These distances are 1.3–2.8 Å longer than those for the 5′-intermediate. Thus, binding of the thymine ring in the large pocket during acylation at the 5′-position is the most likely molecular basis for the high regioselectivity of CAL-B for the 5′-position.

The interaction of the thymine ring with the acyl chain might be the origin of the altered regioselectivity with different acylating agents. An acetyl group would show a smaller interaction than a butanoyl group and indeed the regioselectivity is lower for acetylation as compared to butanoylation (2.7:1

vs. 6.4:1; entries 1 and 2, Table 1). For decanoylation the regioselectivity was lower than for butanoylation (4.0:1 vs. 6.4:1; entries 3 and 2, Table 1), but the hydrophobic side of thymine is much smaller than a decanoyl group and cannot interact with the entire chain. In addition, the larger decanoyl group might crowd the large hydrophobic pocket. The phenyl or benzyl acyl group might make additional π-stacking interactions with thymidine and thereby show higher regioselectivity (40:1 or >75:1; entries 5 and 7, Table 1).

Regioselective CAL-B-catalyzed acylation of 3′,5′-diaminothymidine

CAL-B shows even higher regioselectivity in the acylation of the thymidine analogue, 3′,5′-diamino-3′,5′-dideoxythymidine (**2**, Scheme 2; X = NH).[7b] For example, acetylation of thymidine showed only a 2.7:1 regioselectivity for the 5′-position (entry 1, Table 1) compared to a 17:1 regioselectivity for the 5′-position for acetylation of the amino analogue (entry 1, Table 3). Similarly, the regioselectivity for butanoylation increased from 6.4:1 to >68:1 (compare entry 2, Table 1 and entry 3, Table 3). To avoid chemical acylation, we used unactivated esters as acyl donors and added molecular sieves (4 Å), which accelerated these acylations (Table 3).[22] Varying the concentration of acylating agent did not change the regioselectivity. For the butanoyl, crotonoyl and phenyl moieties, regioselectivity remained high for the 5′-position. For the formylation and acetylation reactions, we always observed mixtures between 5′-acylated and 3′,5′-diacylated compounds in ratios depending on the reaction time.

Table 3. Regioselectivity of CAL-B-catalyzed acylation of 3′,5′-diaminothymidine (**2**) with nonactivated esters.[a]

	Acyl group	R[b]	R1[b]	T [°C]	t [h][c]	5′ [%]	3′, 5′ [%]	5′ Selectivity[d]
1	acetyl	Me	Et	40	6	80	5	17:1
2	formyl	H	Et	40	8	55	20	3.8:1
3	butanoyl	Pr	Et	40	32	68	0	>68:1
4	crotonoyl	MeCH=CH	Me	60	31	83	0	>83:1
5	benzoyl	Ph	Me	60	75	67	0	>67:1

[a] See ref. [7b]. [b] See Scheme 2. [c] Time refers to either the time to reach high conversions or the time after which no further reaction was observed. [d] Selectivity was estimated from the ratio of the 3′ and 5′ monoacylated products plus the amount of double acylation added to each.

Molecular modeling of the CAL-B-catalyzed acylation of 3′,5′-diaminothymidine

Molecular modeling of the normal orientation: Modeling of the CAL-B-catalyzed acetylation of 3′,5′-diamino-3′,5′-dideoxythymidine (**2**, Scheme 2) started with a geometry optimization of the corresponding phosphonamidates,[23] (Scheme 3B, X = NH, R = CH_3; Figures S2 and S3 in the Supporting Information). However, in spite of the similarity of phosphonates and phosphonamidates, the phosphonamidate structures showed longer distances for the key hydrogen bonds a–c (entries 3 and 4, Table 2).[24] In the 5′-intermediate, the longer hydrogen bonds were those between the catalytic His and the nucleophile (3.25 Å) and between the oxyanion and Gln106 (3.27 Å). In the 3′-intermediate, the longer hydrogen bond was between His224 and Ser105 (3.23 Å). Thus, modeling cannot explain the experimentally observed strong preference for the 5′-position.

The origin of these differences in the phosphonate and phosphonamidate structures is likely the lower electronegativity of NH versus O as well as subtle differences in the bond lengths and bond angles in the two structures (P–O bond lengths (1.62 Å) vs. P–N (1.54 Å)). Due to the rigidity of the intermediates, these small differences in bond lengths and angles can make larger differences in the orientation of the substrate (an "arc effect"). Furthermore, the lower electronegativity of the nitrogen atom weakens the hydrogen bond between His224 and the NH group of the nucleoside, and the hydrogen atom of the nucleophile is placed close to His224, the catalytic histidine (Scheme 4).

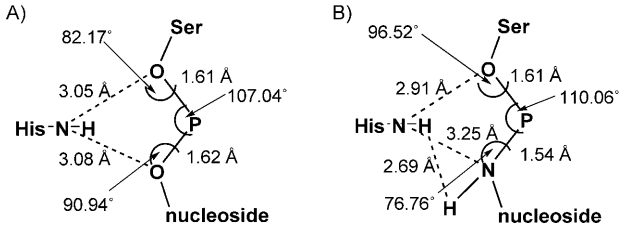

Scheme 4. Comparison of bond angles and lengths in phosphonate and phosphonamidate transition-state analogues. A) The structure for 5′-acylation of thymidine (Figure 2A) shows a symmetrical structure while; B) the intermediate for 5′-acetylation of 3′,5′-diaminothymidine (Figure S2) shows longer P–O than P–N bond lengths. The lower electronegativity of nitrogen weakens the hydrogen bond between His224 and the NH group of the nucleoside (3.25 Å). Furthermore, the hydrogen atom of the nucleophile is placed close to His224, the catalytic histidine.

Two additional destabilizing interactions in the 5′-acetylation intermediate might decrease the difference between the 5′- and 3′-acetylation intermediates. The 5′-acetylation intermediate lacks the hydrophobic interaction between the hydrophobic side of the thymine and the acyl group because this ring does not bind as deeply into the large hydrophobic pocket. Second, the 5′-acetylation intermediate places the polar 3′-NH_2 group near the hydrophobic side chains of Ala281, Leu278 and Trp104 in the medium-size pocket.

Inverse mechanism, overall fit: Since normal orientation models did not explain the increased regioselectivity with the same acylating agents, we considered an inverse orientation in which the acyl chain fits in the medium hydrophobic pocket, and the diaminonucleoside nucleophile fits in the acyl-binding region of the large pocket (Scheme 5). Initially, we focused on the transition state for acylation of the aminonucleoside to test the overall fit of the inverse orientation. This acylation could proceed for the aminolysis reaction without assistance

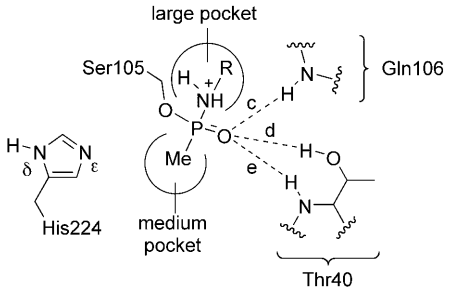

Scheme 5. Inverse orientation of the phosphonamidate transition-state analogue for acylation of 3′,5′-diaminothymidine from the active site of CAL-B. The 3′,5′-diaminothymidine (R-NH_2^+ moiety) lies in the large hydrophobic pocket and the methyl group binds in the medium pocket.

of the catalytic histidine because amines are much more nucleophilic than alcohols. Furthermore, the minor steric hindrance of the diaminonucleoside in the large hydrophobic pocket could favor these structures. Thus, for example, in the inverse structure (Figure 3 A) there are several destabilizing interactions between the nucleoside and three amino acids (Gln157, Ile189 and Ile285) around 4 Å from nucleoside; meanwhile, with the normal orientation (Figure S2 in the Supporting Information), seven amino acids destabilize the intermediate at that distance (Thr40, Trp104, His224, Leu278, Ala281, Ala282, and Ile285).

5′ acetylation catalyzed by CAL-B (favored): The best model of the tetrahedral intermediate for the 5′-*N*-acylation (Figure 3 A) shows the sugar and the thymine moieties in the large hydrophobic pocket with C-4 and N-3 pointing out to the solvent. Four of the six key hydrogen bonds were present while avoiding inter- and intramolecular steric interactions (entry 5, Table 2). The methyl group of the acetate bound in the medium pocket. An interaction between the O-2 carbonyl group of the base and the 5′-amine nucleophile (3.36 Å) might also stabilize this structure (Figure 3 B).

3′ acetylation catalyzed by CAL-B (not favored): In this intermediate, the sugar was placed in the large hydrophobic pocket but the thymine ring did not bind into this subsite and pointed out to the solvent (Figure S4 in the Supporting Information). No structures were found to fit the thymine ring in a hydrophobic region of the catalytic site.

These models for acetylation of the nucleoside could explain the high regioselectivity of CAL-B for acylation of the 5′-amino group. The loss of one of the key hydrogen bonds, in the 3′-phosphonamidate, between the oxyanion and Thr40 (angle $<120°$, entry 6, bond e, Table 2), and better binding of the thymine ring in the 5′-intermediate appear to be a key determinant of the lipase selectivity. Also, the 3′-acylation intermediate lacks an interaction between the O-2 carbonyl group and the nucleophile amine because of its *trans* orientation.

Inverse mechanism, proton transfers: The modeling above showed that the shape of the active site allows an inverse orientation. However, these structures contained only four of the six key hydrogen bonds for catalysis. The role of the missing hydrogen bonds is to transfer a proton from the nucleophile (amine) to the serine. To be plausible as catalytically productive structures, the inverse orientation must provide an alternate path for these proton transfers. Thus, initial attack of the amino nucleoside on the acyl–enzyme intermediate leads to a protonated species, which we mimic as a phosphonamidate (P–NH_2^+–R). In the normal mechanism, the catalytic histidine transfers the proton from the initially protonated species to serine, but this histidine is too far away from the nucleophile in the inverse orientation to allow a direct proton transfer (3.71 Å to N_ε of His224). Direct transfer of the proton from the ammonium group to the oxygen atom of the serine is also unlikely because of an acute angle (N–H–O = 68°).[24] Modeling suggests that a water molecule might aid a stepwise proton transfer.

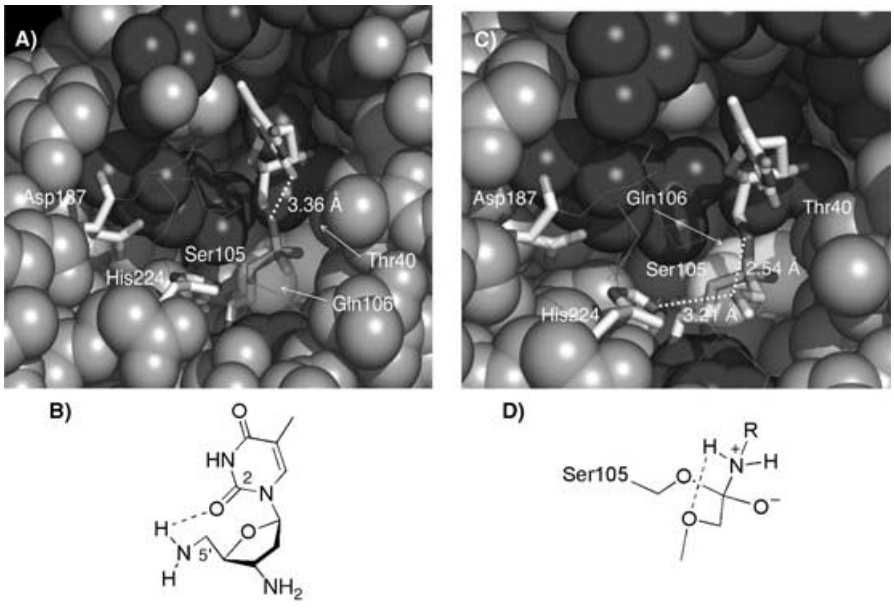

Figure 3. A) Best model of phosphonamidate for 5′-*N*-acetylated intermediate of **2** in the inverse conformation. This tetrahedral intermediate situates the sugar ring and thymine in the large hydrophobic pocket. A potential hydrogen-bond stabilization appears between the O-2 carbonyl group of thymine and the nucleophilic 5′-amino nitrogen atom; B) Detail of the hydrogen bond between the O-2 of the thymine ring and the 5′-NH_2 nucleophile; C) Best model of the amine-protonated intermediate of **2** and the methoxymethyl group with CAL-B in the inverse conformation. The methoxymethyl chain places the oxygen atom between the ammonium group and the N_ε-histidine, making the autocatalyzed transference of the proton possible; D) Possible stabilizing interaction of the methoxymethylene acyl chain in the protonated amine intermediate for the aminolysis.

Previously, modeling suggested that an alcohol could transport a proton between the substrate and the key histidine in the CAL-B-catalyzed enantioselective ring opening of β-lac-

tams.[25] In our case, water could play this role since it remains bound to the lipase even in organic solvents. We modelled a water molecule in several positions near the catalytic triad and found a stable position midway between the protonated amine and the histidine in these inverse phosphonamidate intermediates (Figure 4). The water molecule is about 4 Å from

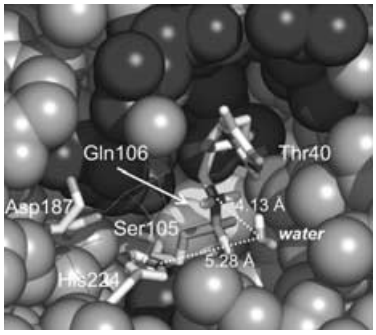

Figure 4. Best model of the N-5′-inverse intermediate of **2** stabilized with a water molecule. This molecule is placed almost equidistant from the nucleophile amine and His224. In this structure the water molecule does not form a hydrogen bond with the protonated amine, but small motions of this water molecule would allow stepwise transfer from the amino group to the histidine or serine. Residues Glu188 and Ile189 are shown in lines for clarity.

the ammonium group and 5 Å from the N_ε-histidine. This position is still too far to hydrogen bond with either group, but small movements of this water molecule would allow stepwise proton transfer from the ammonium moiety to the N_ε of His224 (entry 7, Table 2).

Furthermore, the carbonyl O-2 group was close to the 5′-amino group nitrogen atom (3.41 Å), making the latter more nucleophilic. This interaction has a potential catalytic role since it could replace the activation effect on the amino group due to the N_ε of His224 in the serine mechanism and could be a key reason for the excellent regioselectivity of the lipase. This interaction might also be involved in the proton transfer from the ammonium group to histidine or serine.

Kinetic evidence for an inverse mechanism: A key feature of the proposed inverse mechanism is an interaction between the 5′-NH_2 group and the O-2 carbonyl group of the thymine, which makes that position more nucleophilic. As further evidence for the importance of the interaction between the 5′-NH_2 group and the O-2 carbonyl group of the thymine, we note that diaminonucleosides containing this O-2 carbonyl group (thymidine, 2′-deoxyuridine, (*E*)-5-(2-bromovinyl)-2′-deoxyuridine) undergo N-acylation,[7] while a compound that lacks this O-2 carbonyl group (*N*-benzoyl-2′-deoxyadenosine) does not. However, CAL-B does catalyze the acylation of the corresponding natural purine nucleoside even though it does not contain this O-2 carbonyl group.[6c,d] This difference further suggests that the acylation of alcohols and amines might follow different pathways.

The faster enzymatic aminolysis reactions with methoxyacetate esters as compared to the isosteric butyryl esters[26] are one key to the successful commercialization of a lipase-catalyzed kinetic resolution of amines.[27] Although the inductive effect of the β-oxygen atom to the carbonyl group might contribute to the faster reaction, this explanation is inconsistent with the lack of a similar faster acylation of alcohols.

To the best of our knowledge, there is no explanation for this effect based on the normal orientation of substrates in the active site. However, we hypothesized that the β-oxygen atom could accelerate the reaction of amines if they reacted through an inverse mechanism (Figure 3D). To test this hypothesis, we compared the rates of acylation of nucleoside alcohols and amines using acyl donors with and without β-oxygen atom. We predicted that acyl donors containing a β-oxygen atom should react faster in the acylation of amines than those without because they follow the inverse mechanism, but they should not in the acylation of alcohols because they follow the normal mechanism.

We first compared the initial rates of the CAL-B-catalyzed esterification of natural nucleoside **1** (Scheme 6). We used oximes as acyl donors because they showed the fastest rates

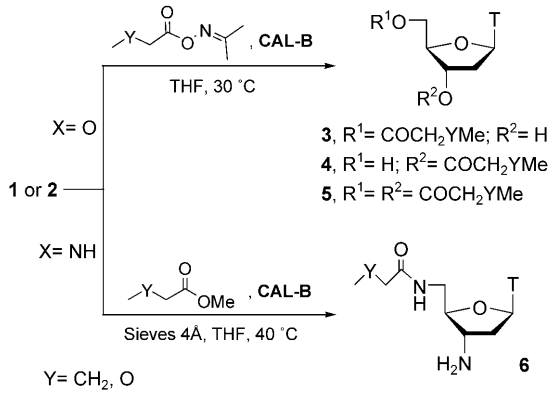

Scheme 6. Regioselective enzymatic acylation of **1** with oxime esters and of **2** with methyl esters.

and best yields in previous work.[6b–g] Short reaction times yielded only 5′- and 3′-acylated products, **3** and **4**, but longer reaction times also yielded 3′,5′-diacylated nucleosides **5**. Both initial rates were similar (slope = 7.9 vs. 8.1) indicating no significant influence by the β-oxygen atom in the acyl chain (Figure 5A). Second, we compared the initial rates of the CAL-B-catalyzed aminolysis of **2** (Scheme 6). We used methyl esters as acyl donors because the oximes also reacted without lipase catalysis.[7] These acylations yielded only 5′-monoacylated nucleosides **6**. The initial rates differed approximately fourfold (slope = 1.4 vs. 4.9) indicated a faster reaction for the acyl donor with a β-oxygen atom in the acyl chain (Figure 5B).[28] This result is consistent with the amine nucleoside **2**, but not natural nucleoside **1**, reacting through an inverse mechanism.

Molecular modeling supports the suggestion that the β-oxygen atom has a catalytic role in the acylation of aminonucleoside **2** through an inverse mechanism. Modeling of the acylation of **2** with a propyl group via an inverse mechanism following the same approach outlined above for acetylation yielded similar structures (Figure S5 in the Supporting Information). The diaminonucleoside fits in the large hydrophobic

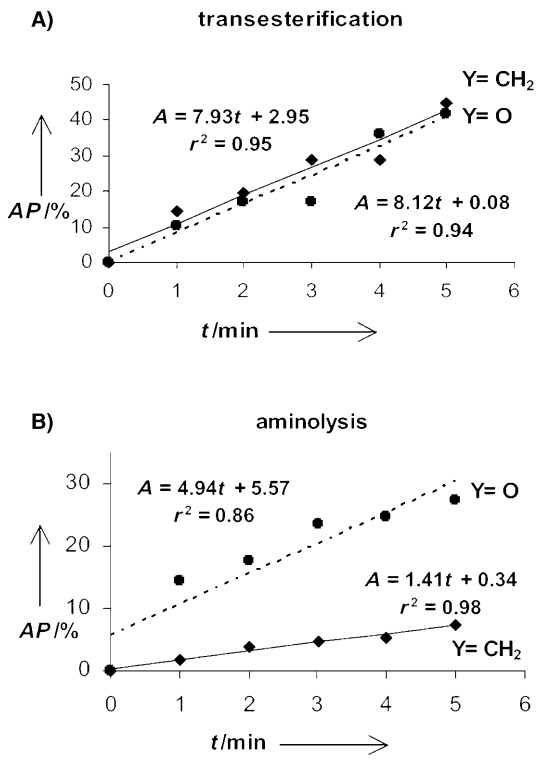

Figure 5. Initial rates of CAL-B catalyzed processes: A) enzymatic transesterification reactions of **1** with oxime butyrate (——) and oxime methoxyacetate (-----) show similar initial rates for both acylating agents; B) enzymatic aminolysis reactions of **2** with methyl butyrate (——) and methyl methoxyacetate (-----) show an approximately fourfold faster initial rate for methyl methoxyacetatate, consistent with a possible catalytic role of this β-oxygen atom in the acylation of amines. AP = area of products.

pocket, while the propyl group fits in the medium subsite. However, modeling of the acylation with the methoxyacetyl group following an inverse mechanism revealed a potential catalytic role of the β-oxygen atom (entry 9, Table 2, Figure 3C). The oxygen atom of the acyl moiety lies close to both the ammonium group (2.54 Å), stabilizing its positive charge, and to N_ε of His224 (3.21 Å). This location is ideal to act as a proton transporter.[29]

Discussion

CAL-B shows excellent regioselectivity for the acylation of natural[6] and non-natural[7] nucleosides toward the chemically more reactive 5′-position. The enzyme's active-site structure influences this regioselectivity. For example, CAL-B was the only biocatalyst that showed high regioselectivity of the 5′-position in 3′,5′-diaminonucleosides, while the lipase from *Pseudomonas cepacia* (PSL-C) favored the 3′-position.[7b] The regioselectivity in aminolysis was much higher than in transesterification reactions (Tables 1 and 3 and Results Section).

For the natural nucleosides (acylation of an alcohol moiety), molecular modeling identified a molecular basis for the observed regioselectivity. Acylation of the 5′-OH binds the thymine base in a hydrophobic pocket, while acylation of the 3′-OH does not. An interaction between the acyl chain and the thymine ring may explain why regioselectivity varies with different acyl groups.

For the 3′,5′-diaminonucleosides, modeling of a normal orientation did not explain the preference for the 5′-NH_2 because in the 5′-intermediate several stabilizing interactions were lost and similar orientations and hydrogen bonds are present in both 3′- and 5′-structures. To explain the observed regioselectivity in 3′,5′-diaminonucleosides, we considered an inverse orientation, which has an opposite binding of the nucleophile and the acyl chain in the active site of the lipase. Bordusa and co-workers proposed an inverse orientation in several protease-catalyzed reactions, but this is the first proposal of an inverse disposition in lipase-catalyzed reactions. Modeling this inverse orientation easily explained the observed regioselectivity. First, the structure for acylation at the slower-reacting 3′-position showed a poorer fit of the thymine ring in the hydrophobic pocket and lacked a key hydrogen bond. On the other hand, the structure for acylation at the faster reacting 5′-position showed a new stabilizing interaction between the carbonyl O-2 group of the thymine and the nucleophile amine, which might have a catalytic role.

In spite of the higher nucleophilicity of amines compared to alcohols, most hydrolase-catalyzed acylations involve alcohols not amines. Further, reactions with amines are often slower, requiring larger amounts of hydrolase or longer reaction times. In this paper, we suggest a possible reason for this difference for the specific case of CAL-B-catalyzed regioselective acylation of natural nucleosides and 3′,5′-diaminonucleosides. Scheme 7 summarizes the proposed inverse mechanism for the aminolysis reaction with CAL-B. Although we have no direct evidence for the proposed mechanism, we have indirect kinetic evidence together with modeling results. We also have no direct or indirect evidence that would rule out this mechanism. The key difference occurs in the second tetrahedral intermediate (TI-2). The amine (nucleophile) attacks directly without histidine activation, creating a zwitterionic structure in which the ammonium group binds into the large hydrophobic pocket, placing the ester chain in the medium subsite (inverse TI-2). Later, a proton transfer (e.g. molecule of water), carries a proton from the ammonium group to the histidine residue (inverse TI-2′), and finally, the subsequent intermediate (inverse TI-2′′) would evolve as usual transferring the proton to the oxygen atom of the serine yielding the corresponding amide.

This reaction through an inverse orientation is an example of catalytic promiscuity.[30] This term means the ability of enzyme active sites to catalyze distinct chemical transformations which may differ in the functional groups involved, that is, the type of bond formed or cleaved during the reaction and/or in the catalytic mechanism or path of bond making and breaking. CAL-B has already demonstrated that it is able to catalyze other types of reactions such as aldol[31] or Michael additions.[32] The inverse substrate orientation proposed in this paper is an example of a different catalytic mechanism for CAL-B. Bocola et al.[33] have previously described the X-ray structure of CAL-B phosphonamidate bound to both enantiomers of 1-phenylethylamine showing normal orientation, but

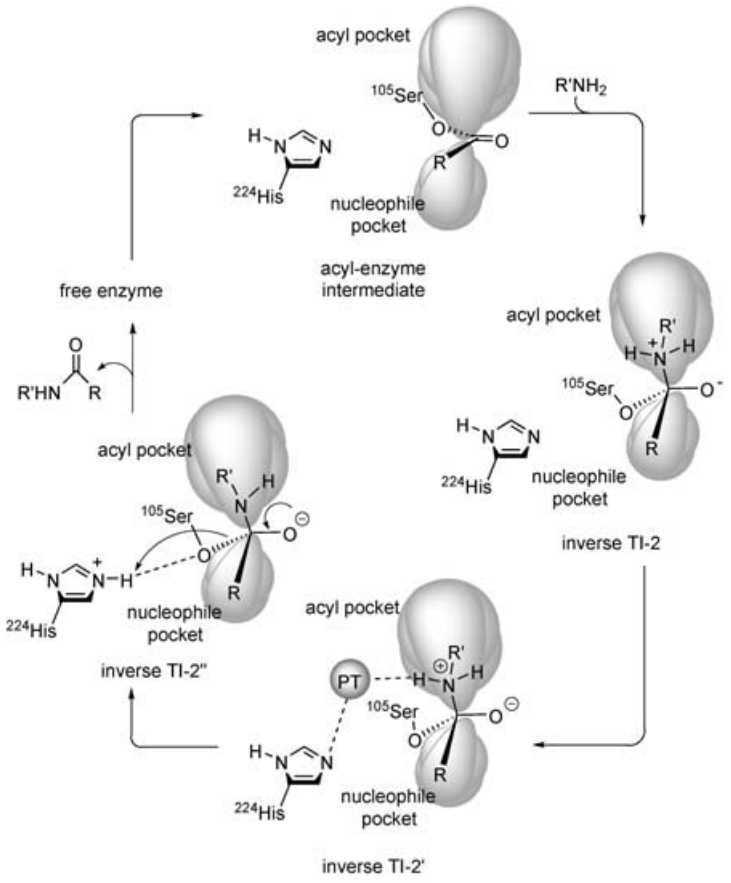

Scheme 7. Inverse mechanism for enzymatic aminolysis reaction with CAL-B.

other X-ray structures for phosphonates showed an inverse orientation.[16,18]

Other examples of an altered catalytic mechanism include: a) reactions after removal of a catalytically essential amino acid residue, which dramatically slows reactions, but does not eliminate them. The remaining less efficient reaction must follow a different path;[34] b) reactions that involve substrate-assisted catalysis, in which the only substrates converted are those that restore the missing functional group so that it can actively participate in catalysis;[35] and c) reactions catalyzed by binding proteins from no bond breaking to some bond breaking. For example, bovine serum albumin catalyzes several types of transformations,[36] myoglobin performs slow oxidations in the presence of hydrogen peroxide,[37] and in several cases a catalytic antibody created to catalyze one reaction can also promote another reaction.[38]

Experimental Section

General: *Candida antarctica* lipase B (CAL-B, Novozym 435, 7300 PLU g^{-1}) was a gift from Novo Nordisk Co. All other reagents were purchased from commercial sources. THF was dried over sodium metal, and pyridine was dried over potasium hydroxyde, they were then distilled under nitrogen.

Molecular modeling: The program InsightII, version 2000.1, was used for viewing the structures. The geometric optimizations were performed by using Discover, version 2.9.7 (Accelrys, San Diego, CA, USA), with the AMBER[39] force field. The distance-dependent dielectric constant was set to 4.0 to mimic the electrostatic shielding of the solvent, and the one-to-four van der Waals interactions were scaled to 50%. The crystal structure for CAL-B (1Lbs[18]) was obtained from the Protein Data Bank (www.rcsb.org/pdb/) and includes a phosphonate. Protein structures in Figures 1–4 were generated by using PyMOL 0.97.

Initial rates of esterification reactions: A solution containing the oxime ester (0.5 mmol) and **1** (48 mg, 0.2 mmol) in THF (2 mL) was prepared in an Erlenmeyer flask. This mixture was transferred to an orbital shaker and shaken (250 rpm) for at least 30 min at 30 °C. Finally, CAL-B (50 mg) was added to the solution, and at regular intervals of 1 min a sample was extracted (100 μL) from the flask (five samples per reaction), the solvent was evaporated, and the sample was silylated by treatment with anhydrous pyridine (50 μL), HMDSA (4 μL), and TMSCl (2 μL). The reaction was carried out in an Eppendorf PCR tube. The mixture was shaken vigorously for about 2 min and was then allowed to stand for 10 min at RT prior to chromatography. The sample was analyzed by gas chromatography on a TRACSIL TRB-5A capillary column (30 m × 0.32 mm × 0.50 μm) with nitrogen as carrier gas and a flame ionization detector. Injector and detector temperatures were set at 300 °C, head column pressure at 14 psi and split 90:1; initial column temperature 220 °C (3 min), rate 5 °C min^{-1} until 260 °C, then 15 min at 260 °C, followed by heating rate 5 °C min^{-1} until 300 °C, final column temperature was 300 °C (10 min). 3′,5′-Di-*O*-TMS-2′-deoxyuridine (as internal standard) eluted at 11.8 min; 5′-*O*-butyryl-3′-*O*-TMS-thymidine[6f] at 15.9 min; 3′-*O*-butyryl-5′-*O*-TMS-thymidine[6g] at 16.3 min; 3′,5′-di-*O*-butyrylthymidine[6f] at 23.1 min; 5′-*O*-methoxyacetyl-3′-*O*-TMS-thymidine at 16.8 min; 3′-*O*-methoxyacetyl-5′-*O*-TMS-thymidine at 17.3 min; 3′,5′-di-*O*-methoxyacetylthymidine at 26.8 min. Standard curves were produced enabling the concentration of the ester product to be followed over time. The spectroscopical data of 5′-*O*-, 3′-*O*-, and 3′,5′-di-*O*-methoxyacetylthymidine are given in the Supporting Information.

Initial rates of aminolysis reactions: A solution containing the methyl ester (0.67 mmol), 3′,5′-diamino-3′,5′-dideoxythymidine (**2**; 20 mg, 0.08 mmol) and molecular sieves (4 Å, 20 mg) in THF (4.5 mL) was prepared in an Erlenmeyer flask. This mixture was transferred to an orbital shaker and shaken (250 rpm) for at least 30 min at 40 °C. Finally, CAL-B (10 mg) was added to the solution, and at regular intervals of 1 min, a sample was extracted (100 μL) from the flask (five samples per reaction) and the solvent evaporated. The samples were then analyzed by HPLC on a Kromasil 100 C18 column (150 × 4.6 mm, 5 μm). HPLC conditions: constant flow: 0.5 mL min^{-1}; temperature: 25 °C; eluent gradient: A/B 1:99 (6 min), then polarity was changed linealy until A/B 20:80 at 15 min, and finally was changed linealy until A/B 100:0 at 25 min, with A = CH_3CN and B = ammonium acetate (0.02 M) in water with 1% CH_3CN. 3′,5′-Diamino-3′,5′-dideoxythymidine[7b,40] elutes at 4.2 and 7.0 min; 3′-amino-5′-butyrylamino-3′,5′-dideoxythymidine[7b] at 18.7 min; 3′-amino-5′-methoxyacetylamino-3′,5′-dideoxythymidine (spectroscopical data is given in the Supporting Information) at 16.6 min.

Acknowledgements

We express our appreciation to Novo Nordisk Co. for the generous gift of CAL-B. Financial support of this work by the Spanish Ministerio de Ciencia y Tecnología (Project PPQ-2001-2683) and by the Principado de Asturias (Project GE-EXP01-03) is gratefully acknowledged. S.F. thanks MCYT for a personal grant (Ramón y Cajal Project). I.L. and J.M. thank MCYT for predoctoral fellowships.

Keywords: aminolysis · biotransformations · enzyme catalysis · molecular modeling · nucleosides

[1] a) M. Ferrero, V. Gotor, *Chem. Rev.* **2000**, *100*, 4319 – 4347; b) M. Ferrero, V. Gotor, *Monatsh. Chem.* **2000**, *131*, 585 – 616.
[2] a) C. M. Galmarini, *Electron. J. Oncol.* **2002**, *1*, 22 – 32; b) R. K. Robins, G. R. Revankar in *Antiviral Drug Development* (Eds.: E. De Clercq, R. T. Walker), Plenum Press, New York, **1998**, p 11; c) T. K. Mansour, R. Storer, *Curr. Pharm. Des.* **1997**, *3*, 227 – 264.
[3] a) S. Czernecki, J. M. Valery in *Carbohydrates in Drug Design* (Eds.: Z. J. Witczak, K. A. Nieforth), Marcel Dekker, New York, **1997**, p 495; b) "Pyrimidine Nucleoside Analogues as Antiviral Agents", E. De Clercq, *NATO ASI Ser. A Life Sci.* **1984**, *73*, 203 – 230.
[4] W. Plunkett, V. Gandhi, *Cancer Chemother. Biol. Response Modif. Annu.* **2001**, *19*, 21 – 45.
[5] E. T. Kool, *Chem. Rev.* **1997**, *97*, 1473 – 1487.
[6] a) J. García, S. Fernández, M. Ferrero, Y. S. Sanghvi, V. Gotor, *Tetrahedron Lett.* **2004**, *45*, 1709 – 1712; b) J. García, S. Fernández, M. Ferrero, Y. S. Sanghvi, V. Gotor, *Org. Lett.* **2004**, *6*, 3759 – 3762; c) J. García, S. Fernández, M. Ferrero, Y. S. Sanghvi, V. Gotor, *Tetrahedron: Asymmetry* **2003**, *14*, 3533 – 3540; d) J. García, S. Fernández, M. Ferrero, Y. S. Sanghvi, V. Gotor, *Nucleosides Nucleotides Nucleic Acids* **2003**, *22*, 1455 – 1457; e) F. Morís, V. Gotor, *Tetrahedron* **1993**, *49*, 10089 – 10098; f) F. Morís, V. Gotor, *J. Org. Chem.* **1993**, *58*, 653 – 660; g) V. Gotor, F. Morís, *Synthesis* **1992**, 626 – 628.
[7] a) I. Lavandera, S. Fernández, M. Ferrero, E. De Clercq, V. Gotor, *Nucleosides Nucleotides Nucleic Acids* **2003**, *22*, 1939 – 1952; b) I. Lavandera, S. Fernández, M. Ferrero, V. Gotor, *J. Org. Chem.* **2001**, *66*, 4079 – 4082.
[8] U. T. Bornscheuer, R. J. Kazlauskas, *Hydrolases in Organic Synthesis*, Wiley-VCH, Weinheim, **1999**.
[9] a) L. Hedstrom, *Chem. Rev.* **2002**, *102*, 4501 – 4523; b) A. R. Fersht, *Enzyme Structure and Mechanism*, 2nd ed., Freeman, New York, **1985**.
[10] a) W. V. Tuomi, R. J. Kazlauskas, *J. Org. Chem.* **1999**, *64*, 2638 – 2647; b) J. Zuegg, H. Hönig, J. D. Schrag, M. Cygler, *J. Mol. Catal. B* **1997**, *3*, 83 – 98; c) M. Cygler, P. Grochulski, R. J. Kazlauskas, J. D. Schrag, F. Bouthillier, B. Rubin, A. N. Serreqi, A. K. Gupta, *J. Am. Chem. Soc.* **1994**, *116*, 3180 – 3186.
[11] K. Tanizawa, Y. Kanaoka, W. B. Lawson, *Acc. Chem. Res.* **1987**, *20*, 337 – 343.
[12] F. Bordusa, D. Ullmann, C. Elsner, H.-D. Jakubke, *Angew. Chem.* **1997**, *109*, 2583 – 2585; *Angew. Chem. Int. Ed. Engl.* **1997**, *36*, 2473 – 2475.
[13] M. Thormann, S. Thust, H.-J. Hofmann, F. Bordusa, *Biochemistry* **1999**, *38*, 6056 – 6062.
[14] R. Günther, A. Stein, F. Bordusa, *J. Org. Chem.* **2000**, *65*, 1672 – 1679.
[15] N. Wehofsky, F. Bordusa, *FEBS Lett.* **1999**, *443*, 220 – 224.
[16] C. Luo, H. Leader, Z. Radic, D. M. Maxwell, P. Taylor, B. P. Doctor, A. Saxena, *Biochem. Pharmacol.* **2003**, *66*, 387 – 392.
[17] H.-C. Shin, D. M. Quinn, *Biochemistry* **1992**, *31*, 811 – 818.
[18] J. Uppenberg, N. Öhrner, M. Norin, K. Hult, G. J. Kleywegt, S. Patkar, V. Waagen, T. Anthonsen, T. A. Jones, *Biochemistry* **1995**, *34*, 16838 – 16851.
[19] a) L. F. García-Alles, V. Gotor, *Biotechnol. Bioeng.* **1998**, *59*, 163 – 170; b) L. F. García-Alles, V. Gotor, *Biotechnol. Bioeng.* **1998**, *59*, 684 – 694.
[20] J. Uppenberg, M. T. Hansen, S. Patkar, T. A. Jones, *Structure* **1994**, *2*, 293 – 308.
[21] We obtained four to six structures for each regioisomer by systematic search of dihedral angles shown in Figure S1 (see Supporting Information), making changes of 30°. From these structures, we chose the one with the lowest energy that kept all the six key hydrogen bonds. This best intermediate was geometry-optimized with further systematic search of a dihedral angle of approximately 10–20°.
[22] An explanation for this effect: I. Lavandera, S. Fernández, M. Ferrero, V. Gotor, *Tetrahedron* **2003**, *59*, 5449 – 5456.
[23] The IUPAC name of this class of derivative is methyl(alkylamido)phosphonates.
[24] To identify hydrogen bonds, a donor–acceptor separation of less than 3.20 Å and a donor–hydrogen–acceptor angle of 120° or greater are required.
[25] S. Park, E. Forró, H. Grewal, F. Fülöp, R. J. Kazlauskas, *Adv. Synth. Catal.* **2003**, *345*, 986 – 995.
[26] a) J. González-Sabín, V. Gotor, F. Rebolledo, *Tetrahedron: Asymmetry* **2004**, *15*, 481 – 488; b) F. Balkenhohl, K. Ditrich, B. Hauer, W. Ladner, *J. Prakt. Chem. Chem-Ztg.* **1997**, *339*, 381 – 384.
[27] F. Balkenhohl, B. Hauer, W. Ladner, U. Pressler, US 5728876, **1996**.
[28] Synthesis of the 5′-methoxyacetylamino derivative was also much faster (2 h) than that of the 5′-butyrylated derivative (32 h).
[29] There are studies in which the proton is transferred from a protonated nucleophile amine through substrate-assistance: N. Díaz, D. Suárez, T. L. Sordo, R. Méndez, J. M. Villacorta, *Eur. J. Org. Chem.* **2003**, 4161 – 4172.
[30] U. T. Bornscheuer, R. J. Kazlauskas, *Angew. Chem.* **2004**, *116*, 6156 – 6165; *Angew. Chem. Int. Ed.* **2004**, *43*, 6032 – 6040.
[31] C. Branneby, P. Carlqvist, A. Magnusson, K. Hult, T. Brinck, P. Berglund, *J. Am. Chem. Soc.* **2003**, *125*, 874 – 875.
[32] O. Torre, I. Alfonso, V. Gotor, *Chem. Commun.* **2004**, 1724 – 1725.
[33] M. Bocola, M. T. Stubbs, C. Sotriffer, B. Hauer, T. Friedrich, K. Dittrich, G. Klebe, *Protein Eng.* **2003**, *16*, 319 – 322.
[34] Y. Romsicki, G. Scapin, V. Beaulieu-Audy, S. Patel, J. W. Becker, B. P. Kennedy, E. Asante-Appiah, *J. Biol. Chem.* **2003**, *278*, 29009 – 29015.
[35] A. Magnusson, K. Hult, M. Holmquist, *J. Am. Chem. Soc.* **2001**, *123*, 4354 – 4355.
[36] a) S. Colonna, N. Gaggero, J. Drabowicz, P. Lyzwa, M. Mikolajczyk, *Chem. Commun.* **1999**, 1787 – 1788; b) G. Klein, J.-L. Reymond, *Bioorg. Med. Chem. Lett.* **1998**, *8*, 1113 – 1116; c) F. Hollfelder, A. J. Kirby, D. S. Tawfik, *Nature* **1996**, *383*, 60 – 62.
[37] D. C. Levinger, J.-A. Stevenson, L.-L. Wong, *J. Chem. Soc. Chem. Commun.* **1995**, 2305 – 2306.
[38] a) A. C. Backes, K. Hotta, D. Hilvert, *Helv. Chim. Acta* **2003**, *86*, 1167 – 1174; b) L. C. James, D. S. Tawfik, *Protein Sci.* **2001**, *10*, 2600 – 2607.
[39] a) W. D. Cornell, P. Cieplak, C. I. Bayly, P. A. Kollmann, *J. Am. Chem. Soc.* **1993**, *115*, 9620 – 9631; b) S. J. Weiner, P. A. Kollman, D. A. Case, U. C. Singh, C. Ghio, G. Alagona, S. Profeta, P. Weiner, *J. Am. Chem. Soc.* **1984**, *106*, 765 – 784.
[40] T.-S. Lin, W. H. Prusoff, *J. Med. Chem.* **1978**, *21*, 109 – 112.

Received: November 26, 2004
Published online on June 24, 2005

